Inorg. Chem. **2002**, *41*, 5100–5106

Synthesis and Characterization of Completely Delocalized Mixed-Valent Dicopper Complexes

Rajeev Gupta,[†] Zhi Hui Zhang,[†] Douglas Powell,[†] Michael P. Hendrich,[‡] and A. S. Borovik*[,†]

Departments of Chemistry, University of Kansas, Lawrence, Kansas 66045, and Carnegie Mellon University, Pittsburgh, Pennsylvania 15213

Received April 24, 2002

The multidentate ligands tris[(*N*′-*tert*-butylureayl)-*N*-ethyl)]amine (H_6**1**) and 1-(*tert*-butylaminocarbonyl)-2,2-dimethylaminoethane (H_2**2**) have been used to investigate the assembly and properties of complexes with $Cu^{1.5}Cu^{1.5}$ units. The complexes $[Cu(H_5\mathbf{1})]_2^{+}$ and $[Cu(H\mathbf{2})]_2^{+}$ have been isolated and structurally characterized by X-ray diffraction methods. $[Cu(H_5\mathbf{1})]_2^{+}$ has a $Cu^{1.5}Cu^{1.5}$ core, with each copper ion having square planar coordination geometry. The copper ions are linked through two mono-deprotonated urea ligands, which coordinate as μ-1,3-(κN:κO) ureate bridges to produce a Cu–Cu distance of 2.39 Å. The remaining two urea arms of $[H_5\mathbf{1}]^{-}$ form intramolecular hydrogen bonds, the result of which is to confine the $Cu^{1.5}Cu^{1.5}$ unit within a pseudomacrocycle. The structure of $[Cu(H\mathbf{2})]_2^{+}$ lacks intramolecular hydrogen bonds and thus does not have a pseudomacrocyclic structure. However, the structural properties of the $Cu^{1.5}Cu^{1.5}$ core in $[Cu(H\mathbf{2})]_2^{+}$ are nearly identical to those of $[Cu(H_5\mathbf{1})]_2^{+}$. Both complexes exhibit rhombic EPR spectra at 77 K, which do not change upon cooling to 4 K. The optical spectra of $[Cu(H_5\mathbf{1})]_2^{+}$ and $[Cu(H\mathbf{2})]_2^{+}$ are dominated by an intense band at ~700 nm. These spectral characteristics are consistent with $[Cu(H_5\mathbf{1})]_2^{+}$ and $[Cu(H\mathbf{2})]_2^{+}$ being classified as fully delocalized (type III) mixed-valent species.

Introduction

A variety of mixed-valent $Cu^{I}Cu^{II}$ complexes have been reported. Most examples are type I systems,[1] where the unpaired electron is localized on one metal center.[2] There are far fewer examples of type II and type III $Cu^{I}Cu^{II}$ complexes. Synthetic type II systems have only been reported for complexes with Robson's-type macrocyclic binucleating ligands.[3] Type III $Cu^{1.5}Cu^{1.5}$ complexes, where the unpaired electron is delocalized between the two copper ions at all temperatures, are limited to those with octaazacryptand,[4] (*N*-thioethyl)daco,[5] and μ-1,3-carboxylate ligands.[6] In addition to these synthetic species, the Cu_A site in cytochrome *c* oxidase[7] and the active site in nitrous oxide reductase[8] contain fully delocalized mixed-valent $Cu^{1.5}Cu^{1.5}$ centers. The unique electronic and functional properties of these sites have been attributed to the presence of a short Cu−Cu bond (~2.5 Å), which appears to be characteristic of type III $Cu^{1.5}Cu^{1.5}$ centers.

We have introduced the tripodal ligand tris[(*N*′-*tert*-butylureayl)-*N*-ethyl)]amine (H_6**1**), which has three *N*-

* Author to whom correspondence should be addressed. E-mail: aborovik@ukans.edu.
[†] University of Kansas.
[‡] Carnegie Mellon University.

(1) Robin, M. B.; Day, P. *Adv. Inorg. Chem. Radiochem.* **1967**, *10*, 247−422.
(2) Dunaj-Jurco, M.; Ondrejovic, G.; Melnik, M.; Garaj, J. *Coord. Chem. Rev.* **1988**, *83*, 1−28.
(3) (a) Gagné, R. R.; Koval, C. A.; Smith, T. J.; Cimolino, M. C. *J. Am. Chem. Soc.* **1979**, *101*, 4571−4580. (b) Long, R. C.; Hendrickson, D. N. *J. Am. Chem. Soc.* **1983**, *105*, 1513−1521.
(4) (a) Harding, C.; McKee, V.; Nelson, J. *J. Am. Chem. Soc*. **1991**, *113*, 9684−9685. (b) Barr, M. E.; Smith, P. H.; Antholine, W. E.; Spencer, B. *J. Chem. Soc., Chem. Commun.* **1993**, 1649−1652. (c) Harding, C.; Nelson, J.; Symons, M. C. R.; Wyatt, J. *J. Chem. Soc., Chem. Commun.* **1994**, 2499−2500. (d) Farrar, J. A.; McKee, V.; R Al-Obaidi, A. H.; McGarvey, J. J.; Nelson, J.; Thomson, A. J. *Inorg. Chem.* **1995**, *34*, 1302−1303.
(5) Houser, R. P.; Young, V. G., Jr.; Tolman, W. B. *J. Am. Chem. Soc.* **1996**, *118*, 2101−2102.
(6) (a) LeCloux, D. D.; Davydov, R.; Lippard, S. J. *J. Am. Chem. Soc.* **1998**, *120*, 6810−6811. (b) LeCloux, D. D.; Davydov, R.; Lippard, S. J. *Inorg. Chem.* **1998**, *37*, 6814−6826. (c) He, C.; Lippard, S. J. *Inorg. Chem.* **2000**, *39*, 5225−5231. (d) Lo, S. M.-F.; Chui, S. S.-F.; Shek, L.-Y.; Lin, Z.; Zhang, X. X.; Wen, G.; Williams, I. D. *J. Am. Chem. Soc.* **2000**, *122*, 6293−6294. (e) Zhang, X.-M.; Tong, M.-l.; Chen, Z.-M. *Angew. Chem., Int. Ed.* **2002**, *41*, 1029−1031.
(7) (a) Iwata, S.; Ostermeier, C.; Ludwig, B.; Michel, H. *Nature* **1995**, *376*, 660−669. (b) Tsukihara, T.; Aoyama, H.; Yamashita, E.; Tomizaki, T.; Yamaguchi, H.; Shinzawa-Itoh, K.; Nakashima, R.; Yaono, R.; Yoshikawa, S. *Science* **1995**, 1069−1074. (c) Lappalainen, P.; Aasa, R.; Malmström, B. G.; Saraste, M. *J. Biol. Chem.* **1993**, *268*, 26416−26421.
(8) Brown, K.; Tegoni, M.; Prudêncio, M.; Pereira, A. S.; Besson, S.; Moura, J. J.; Moura, I.; Cambillau, C. *Nat. Struct. Biol.* **2000**, *7*, 191−195.

10.1021/ic0202918 CCC: $22.00
Published on Web 09/10/2002

ethylene-*N*′-*tert*-butyl urea arms attached to an apical nitrogen atom.[9] During our investigations of its metal-ion-binding

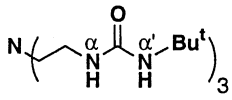

H_6**1**

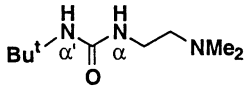

H_2**2**

properties, we found that treating H_6**1** with Cu^I salts in the presence of an oxidant produces a fully delocalized mixed-valent copper ($Cu^{1.5}Cu^{1.5}$) dimer. A similar type III copper dimer can be isolated with the bidentate ligand [H**2**]$^-$. These results suggest that the assembly of a $Cu^{1.5}Cu^{1.5}$ core with this class of ligand is dependent on the two μ-1,3-(κN:κO)-ureate bridges, which separate the copper centers by 2.39 Å. One noteworthy structural feature of the $[CuH_5\mathbf{1}]_2^+$ complex is the confinement of its Cu−Cu core within a pseudomacrocycle formed by intramolecular H-bonds formed from urea groups on adjacent $[H_5\mathbf{1}]^-$ ligands.

Experimental Section

Preparative Methods and Syntheses. All reagents were purchased from commercial sources and used as received, unless otherwise stated. Anhydrous solvents were purchased from Aldrich. Dioxygen was dried on a Drierite gas purifier that was purchased from Fisher Scientific. The syntheses of all metal complexes were performed in a Vacuum Atmospheres drybox under an argon atmosphere. The synthesis of H_6**1** used the method reported previously.[9d]

1-(*tert*-Butylaminocarbonyl)-2,2-dimethylaminoethane ($H_2$2). A diethyl ether (10 mL) solution of 2,2-dimethyl-1,2-ethylenediamine (1.000 g, 11.34 mmol) was treated with *tert*-butylisocyanate (1.123 g, 11.34 mmol) dissolved in 10 mL of diethyl ether. The resulting solution was stirred overnight under a N_2 atmosphere, after which volatiles were removed under reduced pressure. The resultant white solid was flitered off, washed with cold *n*-hexane, and dried under vacuum to afford 1.9 g (91%) of H_2**2**. ^{1}H NMR ($CDCl_3$, ppm): 1.32 (s, 9 H, C(CH_3)$_3$); 2.22 (s, 6 H, N(CH_3)$_2$); 2.39 (t, 2 H, −NCH_2−); 3.18 (m, 2 H, −CH_2NH−); 5.05 (t, 1 H, C(O)NH−) and 5.23 (s, 1 H, C(O)NH−). ^{13}C NMR ($CDCl_3$): δ 29.9 (C(*C*H$_3$)$_3$); 38.5 (−*C*H$_2$NH-); 45.64 (N(*C*H$_3$)$_3$); 50.38 (m, −N*C*H$_2$−); 59.91 (*C*(CH$_3$)$_3$); 158.8 (*C*═O). IR (Nujol, cm^{-1}) ν(NH) 3353, 3318, 3207, 3122, 3050 (urea, s); ν(C−H) 2815, 2784, 2763 (*t*-Bu, m); ν(CO) 1632, 1569 (urea, s). FAB(+)-MS (CH_2Cl_2): 188.3 (MH$^+$). Mp: 67−68 °C.

[Cu(H$_5$1)]$_2$BF$_4$·CH$_2$Cl$_2$. Under an argon atmosphere, a 15 mL CH_2Cl_2 solution of H_6**1** (0.200 g, 0.451 mmol) was treated with [Cu(MeCN)$_4$]BF$_4$ (0.142 g, 0.451 mmol), as a solid in one portion. After stirring this colorless solution for 0.5 h, dry O_2 (11 mL, 0.45 mmol) or [Fe(Cp)$_2$]BF$_4$ (0.062 g, 0.23 mmol) was added, which resulted in the immediate formation of a dark blue solution. This reaction mixture was stirred for 1 h, after which the remaining O_2 was removed under reduced pressure. The solution was filtered through a porous frit, and the filtrate was layered with diethyl ether under argon. This produced a dark-blue microcrystalline compound, which was filtered, washed with diethyl ether, and dried under vacuum to yield 0.19 g (72%) of [Cu(H$_5$**1**)]$_2$BF$_4$. Anal. Calcd (found) for $C_{43}H_{90}N_{14}O_6BCl_2F_4Cu_2$ (includes one CH_2Cl_2): C, 43.56 (43.71); H, 7.60 (7.57); N, 16.55 (17.13). FTIR (Nujol, cm^{-1}): ν(NH) 3406, 3315 (urea, s); ν(CO) 1567 (urea, s); ν(BF$_4^-$) 1060 (split). FAB-MS (CH_2Cl_2): 1010 ([Cu(H$_5$**1**)]$_2^+$). UV/vis (CH_2Cl_2, λ_{max}, nm (ϵ, M^{-1} cm^{-1})): 705 (4000), 568 (1400), 466 (1600), 288 (4870). μ_{eff} (solid, 296 K): 2.00 μ_B. CV (THF, 100 mV s^{-1}): E_{pc} = −1.07 and E_{pa} = 0.33 V vs SCE.

Another method was used to prepare [Cu(H$_5$**1**)]$_2$BF$_4$. A magnetically stirred solution of H_6**1** (0.10 g, 0.23 mmol) in 10 mL of THF was treated with Cu(OAc)$_2$ (0.021 g, 0.11 mmol) under argon. After 30 min the reaction mixture was allowed to react with [Cu(MeCN)$_4$]-BF$_4$ (0.036 g, 0.11 mmol). The resulting deep blue solution was stirred for 1 h at room temperature, after which volatiles were removed under reduced pressure. The crude salt [Cu(H$_5$**1**)]$_2$BF$_4$ was washed with diethyl ether and recrystallized by layering a THF solution of [Cu(H$_5$**1**)]$_2$BF$_4$ with diethyl ether. This afforded the pure salt in 62% (0.083 g) yield.

[Cu(H2)]$_2$BF$_4$ was prepared following the method described above for [Cu(H$_5$**1**)]$_2$BF$_4$ using 0.200 g (1.07 mmol) of H_2**2** and 0.336 g (1.07 mmol) of [Cu(MeCN)$_4$]BF$_4$. The dark blue microcrystalline salt [Cu(H**2**)] $_2$BF$_4$ was isolated in 70% (0.22 g) yield. Anal. Calcd (found) $C_{18}H_{40}N_6O_2BF_4Cu_2$: C, 36.85 (37.16); H, 6.83 (7.15); N, 14.33 (14.30). FTIR (Nujol, cm^{-1}): ν(NH) 3405, 3332, and 3178 (urea, s); ν(CO) 1565 (urea, s); ν (BF$_4^-$) 1060 (split). UV/vis (CH_2Cl_2, λ_{max}, nm (ϵ, M^{-1} cm^{-1})): 672 (4420), 549 (1170), 446 (1295), 360 (sh, 325), 297 (4470). μ_{eff} (solid, 296 K): 1.94 μ_B. CV (THF, 100 mV s^{-1}): E_{pc} = −1.0 and E_{pa} = 0.71 V vs SCE.

[Cu(H**2**)]$_2$BF$_4$ was also synthesized using Cu^I and Cu^{II} precursors as described above for [Cu(H$_5$**1**)]$_2$BF$_4$, using 0.15 g (0.80 mmol) of H_2**2**, 0.073 g (0.40 mmol) of Cu(OAc)$_2$, and 0.13 g (0.40 mmol) of [Cu(MeCN)$_4$]BF$_4$. [Cu(H**2**)]$_2$BF$_4$ was isolated in 75% (0.18 g) yield after recrystallization.

Physical Methods. Electronic spectra were recorded with a Cary 50 spectrophotometer. FTIR spectra were collected on a Mattson Genesis series FTIR instrument and are reported in wavenumbers. NMR experiments were performed on a Bruker Avance DRX-400 MHz spectrometer. Room temperature magnetic susceptibility measurements of solid samples were obtained using a MSB-1 magnetic susceptibility balance (Johnson Matthey). Diamagnetic corrections were taken from those reported by O'Connor.[10] X-band EPR spectra were collected using a Bruker EMX spectrometer equipped with an ER041XG microwave bridge and an Oxford EPR 900 cryostat for measurements at 4 K. A quartz liquid nitrogen finger-dewar (Wilmad Glass) was used to record spectra at 77 K.

Cyclic voltammetric experiments were collected using a BAS CV 50W (Bioanalytical System Inc., West Lafayette, IN) voltammetric analyzer following methods previously reported.[11] Cyclic voltammograms (CV) were obtained using a three-component system consisting of a glassy-carbon working electrode, a platinum wire auxiliary electrode and a glass encased nonaqueous silver−silver nitrate reference electrode containing a Vycor plug to separate it from the bulk solution. Scan rates of between 0.01 and 1.0 V s^{-1} were used to acquire the CV. Anhydrous THF was obtained

(9) (a) Hammes, B. S.; Young, V. G., Jr.; Borovik, A. S. *Angew. Chem., Int. Ed.* **1999**, *38*, 666−669. (b) Shirin, Z.; Hammes, B. S.; Young, V. G., Jr.; Borovik, A. S. *J. Am. Chem. Soc.* **2000**, *122*, 1836−1837. (c) MacBeth, C. E.; Golombek, A. P.; Young, V. G., Jr.; Yang, C.; Kuczera, K.; Hendrich, M. P.; Borovik, A. S. *Science* **2000**, *289*, 938−941. (d) MacBeth, C. E.; Hammes, B. S.; Young, V. G., Jr.; Borovik, A. S. *Inorg. Chem.* **2001**, *40*, 4733−4741. (e) Gupta, R.; MacBeth, C. E.; Young, V. G., Jr.; Borovik, A. S. *J. Am. Chem. Soc*. **2002**, *124*, 1136−1137.

(10) O'Connor, C. J. *Prog. Inorg. Chem.* **1982**, *29*, 203−283.

(11) Ray, M.; Hammes, B. S.; Yap, G. P. A.; Rheingold, Liable-Sands, L. A.; Borovik, A. S. *Inorg. Chem.* **1998**, *37*, 1527−1533.

from Aldrich Chemical Co. and used without further purification. Bu_4NPF_6 was used as the supporting electrolyte and was recrystallized from THF/diethyl ether. A ferrocenium/ferrocene couple was used to monitor the reference electrode and was observed at 0.17 V vs $Ag^{+/0}$ in THF. IR compensation was achieved before each CV was recorded. Potentials are reported versus the saturated calomel couple.

Crystallographic Structural Determination. Intensity data for the compounds were collected using a Bruker SMART APEX CCD area detector mounted on a Bruker D8 goniometer using graphite-monochromated Mo Kα radiation ($\lambda = 0.71073$ Å). The data were collected at 100(2) K. The CCD detector was operated in the 512 × 512 mode and positioned 5.04 cm from the each sample, unless otherwise noted. Each salt is a member of the triclinic space group $P\bar{1}$, which was determined by systematic absences and statistical tests and verified by subsequent refinement. The data for each crystal were corrected for absorption by the semiempirical method from equivalent reflections.[12] Lorentz and polarization corrections were applied. Each structure was solved by direct methods and refined by full-matrix least-squares methods on F^2. Hydrogen atom positions were initially determined by geometry and refined by a riding model. Non-hydrogen atoms were refined with anisotropic displacement parameters. Individual experimental data for each of the salts are discussed in the following paragraphs.

$[Cu(H_51)]_2BF_4 \cdot 2CH_2Cl_2$. The intensity data were measured as a series of ω oscillation frames each of 0.3° for 45 s/frame. Coverage of unique data was 99.2% complete to 26.00° in θ. Cell parameters were determined from a least-squares fit of 3243 peaks in the range $2.34° < \theta < 24.84°$. From 111 peaks that were measured at both the beginning and end of data collection, the crystal showed a decay of −0.07%. The data were merged to form a set of 12253 independent data with $R(\text{int}) = 0.0667$. A total of 676 parameters were refined against 6 restraints to give $wR(F^2) = 0.1712$ and $S = 0.945$ for weights of $w = 1/[\sigma^2(F^2) + (0.0700P)^2]$, where $P = [F_o^2 + 2F_c^2]/3$. The final $R(F)$ was 0.0687 for the 5994 observed, $[F > 4\sigma(F)]$, data. The largest shift/s.u. (s.u. ≡ standard uncertainty) was 0.00 in the final refinement cycle. The final difference map had maxima and minima of 1.186 and −0.915 e/Å^3, respectively.

$[Cu(H2)]_2BF_4$. The intensity data were measured as a series of ω oscillation frames each of 0.25° for 45 s/frame. Coverage of unique data was 99.3% complete to 26.00° in θ. Cell parameters were determined from a least-squares fit of 2175 peaks in the range $2.50° < \theta < 25.89°$. From 69 peaks that were measured at both the beginning and end of data collection, the crystal showed a decay of 0.02%. The data were merged to form a set of 10194 independent data with $R(\text{int}) = 0.0804$. A total of 595 parameters were refined against 10194 data to give $wR(F^2) = 0.1299$ and $S = 0.981$ for weights of $w = 1/[\sigma^2(F^2) + (0.0280P)^2]$, where $P = [F_o^2 + 2F_c^2]/3$. The final $R(F)$ was 0.0649 for the 5417 observed, $[F > 4\sigma(F)]$, data. The largest shift/s.u. was 0.001 in the final refinement cycle. The final difference map had maxima and minima of 0.985 and −0.668 e/Å^3, respectively.

Results and Discussion

Preparation of $[Cu(H_51)]_2^+$. The synthesis of this complex is outlined in Scheme 1. Treating a methylene chloride solution of H_61 with a Cu^I salt afforded a nearly colorless solution. The addition of dioxygen (or $FeCp_2^+$) to the reaction mixture immediately produced a dark blue solution. Purification was achieved by recrystallization to yield the mixed-valent complex, $[Cu(H_51)]_2^+$. Dioxygen and ferrocenium

Scheme 1

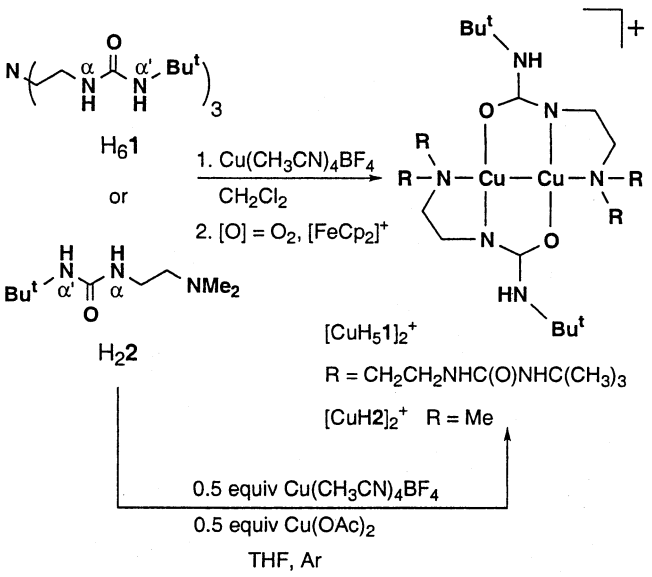

appear to function as outer-sphere oxidants. For instance, we have not detected a dioxygen adduct during the formation of the $[Cu(H_51)]_2^+$. Moreover, the $Cu^{1.5}Cu^{1.5}$ core can also be assembled in the absence of oxidant by treating 1 equiv of H_61 with equal amounts (0.5 equiv) of $Cu(OAc)_2$ and $Cu(CH_3CN)_4BF_4$ (Scheme 1).

The synthesis of $[Cu(H_51)]_2^+$ does not include an external base. This differs from the preparation of the previously reported complexes with H_61, where deprotonation of the urea αNH groups with a base was required for metal ion binding.[9] The absence of base in the formation of $[CuH_51]^+$ is reminiscent of the Cu^{II} assisted deprotonation of amides, where $Cu-N_{amide}$ bonds are readily formed without the aid of an additional base.[13] This binding has been attributed to the large ligand field stabilization energy gained by forming $Cu-N_{amide}$ bonds, which offsets the endothermicity of deprotonating amides. Similar thermodynamic effects may also pertain to urea groups. Consistent with this notion is our inability to prepare complexes of the late 3d metal ions using the synthetic methods in Scheme 1; these methodologies only were successful in preparing dicopper complexes.

$[Cu(H_51)]_2^+$ and $[Cu(H2)]_2^+$ have limited stability before isolation from the reaction mixture. The complexes decompose to intractable species if left for 3 days. The presence of HBF_4, a byproduct of the reactions, or water may cause the instability. This idea is supported by the isolation of a small amount (<10%) of crystalline $[H_32]BF_4$, where the cation is formed by protonation of the apical nitrogen. This salt, whose structure was confirmed by an X-ray diffraction study (Figure S1, Supporting Information), would be a likely product from the decomposition of $[Cu(H2)]_2^+$ by HBF_4. The stabilities of $[Cu(H_51)]_2^+$ and $[Cu(H2)]_2^+$ increase after isolation. These complexes are stable for weeks when stored in the solid state under anhydrous conditions.

(12) Sheldrick, G. M. *SADABS. Program for Empirical Absorption Correction of Area Detector Data*; University of Göttingen: Göttingen, Germany, 1996.
(13) Fabbrizzi, L.; Licchelli, M.; Pallavicini, P.; Perotti, A.; Taglietti, A.; Sacchi, D. *Chem Eur. J.* **1996**, *2*, 75−82 and references therein.

Table 1. Crystallographic Data for $[Cu(H_5\mathbf{1})]_2BF_4\cdot 2CH_2Cl_2$ and $[Cu(H\mathbf{2})]_2BF_4$

	$[Cu(H_5\mathbf{1})]_2BF_4\cdot 2CH_2Cl_2$	$[Cu(H\mathbf{2})]_2BF_4$
molecular formula	$C_{44}H_{92}BCl_4Cu_2F_4N_{14}O_6$	$C_{18}H_{40}BCu_2F_2N_6O_2$
fw	1269.01	586.45
T (K)	100(2)	100(2)
space group	$P\bar{1}$	$P\bar{1}$
a (Å)	12.6003(10)	11.2199(17)
b (Å)	15.9144(13)	11.7721(17)
c (Å)	16.9582(14)	20.188(3)
α (deg)	76.875(2)	97.184(3)
β (deg)	87.667(2)	100.535(3)
γ (deg)	71.452(2)	90.471(3)
Z	2	4
V (Å^3)	3137.9(4)	2599.6(7)
ρ_{calcd} (Mg/m^3)	1.343	1.498
R^a	0.0687	0.0649
$R_w{}^b$	0.1712	0.1299
GOF^c	0.945	0.981

^{a} $R = [\sum|\Delta F|/\sum|F_o|]$. ^{b} $R_w = [\sum\omega(\Delta F)^2/\sum\omega F_o^2]$. ^{c} Goodness of fit on F^2.

Molecular Structure $[Cu(H_5\mathbf{1})]_2BF_4\cdot 2CH_2Cl_2$. Crystal, data collection, and refinement parameters for $[Cu(H_5\mathbf{1})]_2BF_4\cdot 2CH_2Cl_2$ are given in Table 1, and selected distances and angles are presented in Table 2. Additional structural parameters are provided in the Supporting Information. Single crystals of $[Cu(H_5\mathbf{1})]_2BF_4\cdot 2CH_2Cl_2$ belong to the triclinic space group $P\bar{1}$. The salt crystallized with two independent, but structurally similar, cations in the asymmetric unit (referred to as "a" and "b"), where $[Cu(H_5\mathbf{1a})]_2^+$ and $[Cu(H_5\mathbf{1b})]_2^+$ sit on centers of symmetry.

The molecular structure of $[Cu(H_5\mathbf{1a})]_2^+$ is present in Figure 1. Square planar coordination geometry is observed for each metal in the dimer. Donor atoms from the $[H_5\mathbf{1}]^+$ ligands occupy three of the coordination sites on the coppers; the adjoining copper unit fills the fourth site. The apical nitrogen atoms from the $[H_5\mathbf{1}]^+$ ligands coordinate to separate copper ions, with an average $Cu-N_{amine}$ distance of 2.125(4) Å.

One urea arm from each $[H_5\mathbf{1}]^-$ ligand bridges between the copper centers to form two μ-1,3-(κN:κO)-ureate linkages. In this binding mode, the αN^- atom coordinates to one copper ion, while the carbonyl oxygen atom binds to the other metal center. The average $Cu-O_{urea}$ and $Cu-N_{urea}$ bond distances are 1.888(3) and 1.870(3) Å. On each copper, the urea oxygen and nitrogen atoms are positioned nearly trans to one another, the average $N_{urea}-Cu-O_{urea}$ angle being 175.85(18)°. μ-1,3-(κN:κO)-Ureate bridges are rare, with previous examples including $[Fe^{III}_2(\mu\text{-}O)\{\mu\text{-}1,3\text{-}(\kappa N{:}\kappa O)\text{-}OC(NH)NH_2\}(tpa)]^{3+}$ (tpa, tris(pyridylmethyl)amine),[14] $[Ni^{II}_2\{\mu\text{-}1,3\text{-}(\kappa N{:}\kappa O)\text{-}OC(NH)NH_2\}L]^{3+}$ (L, 3,2-bis{bis[2-(diethylamino)ethyl]aminomethyl}pyrazolate),[15] and $Cr_2[\mu\text{-}1,3\text{-}(\kappa N{:}\kappa O)\text{-}OC(NPh)NHPh]\cdot 2THF$.[16,17] The relative paucity of examples for this binding mode of urea is somewhat surprising because a 1,3-ureate bridge is structurally similar to a 1,3-carboxylato bridge, which is prevalent in transition metal chemistry.

Table 2. Selected Bond Distances and Angles for $[Cu(H_5\mathbf{1})]_2^+$ and $[Cu(H\mathbf{2})]_2^+$

distances (Å)		angles (deg)	
		$[Cu(H_5\mathbf{1a})]_2^+$	
Cu1a−N1a	2.118(5)	N1a−Cu1a−N2a	86.37(18)
Cu1a−N2a	1.874(4)	N1a−Cu1a−Cu1a′	172.32(13)
Cu1a−O1a′	1.892(4)	N1a−Cu1a−O1a′	97.38(17)
Cu1a−Cu1a′	2.3898(14)	N2a−Cu1a−O1a′	176.12(19)
		N2a−Cu1a−Cu1a′	86.24(15)
		O1a′−Cu1a−Cu1a′	90.05(12)
		$[Cu(H_5\mathbf{1b})]_2^+$	
Cu1b−N1b	2.131(4)	N1b−Cu1b−N2b	86.27(19)
Cu1b−N2b	1.866(5)	N1b−Cu1b−Cu1b′	171.94(14)
Cu1b−O1b′	1.883(4)	N1b−Cu1b−O1b′	97.67(17)
Cu1b−Cu1b′	2.3978(13)	N2b−Cu1b−O1b′	175.57(17)
		N2b−Cu1b−Cu1b′	86.10(14)
		O1b′−Cu1b−Cu1b′	90.05(11)
		$[Cu(H\mathbf{2a})]_2^+$	
Cu1a−N11a	2.087(5)	N11a−Cu1a−N8a	86.6(2)
Cu1a−N8a	1.869(5)	N11a−Cu1a−Cu1b	170.72(15)
Cu1a−O7b	1.867(5)	N11a−Cu1a−O7b	98.8(2)
Cu1a−Cu1b	2.3876(12)	N8a−Cu1a−O7b	173.4(2)
Cu1b−N11a	2.080(5)	N8a−Cu1a−Cu1b	84.66(15)
Cu1b−N8a	1.858(5)	O7b−Cu1a−Cu1b	90.11(14)
Cu1b−O7a	1.852(4)	N11b−Cu1b−N8b	86.6(2)
		N11b−Cu1b−Cu1a	170.13(15)
		N11b−Cu1b−O7a	95.9(2)
		N8b−Cu1b−O7a	177.5(2)
		N8b−Cu1b−Cu1a	85.90(15)
		O7a−Cu1b−Cu1a	91.62(17)
		$[Cu(H\mathbf{2c})]_2^+$	
Cu1c−N11c	2.079(5)	N11c−Cu1c−N8c	86.6(2)
Cu1c−N8c	1.863(5)	N11c−Cu1c−Cu1c′	170.50(16)
Cu1c−O7c′	1.875(4)	N11c−Cu1c−O7c′	97.1(2)
Cu1c−Cu1c′	2.3765(16)	N8c−Cu1c−O7c′	175.7(2)
		N8c−Cu1c−Cu1c′	86.15(16)
		O7c′−Cu1c−Cu1c	90.34(14)
		$[Cu(H\mathbf{2d})]_2^+$	
Cu1d−N11d	2.084(5)	N11d−Cu1d−N8d	86.6(2)
Cu1d−N8d	1.859(5)	N11d−Cu1d−Cu1d′	171.40(16)
Cu1d−O7d′	1.854(4)	N11d−Cu1d−O7d′	97.6(2)
Cu1d−Cu1d′	2.3824(16)	N8d−Cu1d−O7d′	175.4(2)
		N8d−Cu1d−Cu1d′	86.57(16)
		O7d′−Cu1d−Cu1d	89.46(14)

The presence of two μ-1,3-(κN:κO)-ureate bridges in $[Cu(H_5\mathbf{1})]_2^+$ results in an average Cu−Cu distance of 2.3938(13) Å. This is consistent with a strong metal−metal bond between the copper centers. Moreover, the Cu−Cu separation of ∼2.39 Å found in $[Cu(H_5\mathbf{1})]_2^+$ is comparable to distances reported for $Cu^{1.5}Cu^{1.5}$ complexes containing either octaazacryptands[4] or 1,3-μ-carboxylato bridges,[6] but is significantly shorter than the distance found in the mixed-valent complex with (*N*-thioethyl)daco, which has a Cu···Cu separation of 2.9306(9) Å.[5]

The two noncoordinating urea arms from each tripodal ligand in $[Cu(H_5\mathbf{1})]_2^+$ form intramolecular hydrogen bonds on both sides of the $Cu^{1.5}Cu^{1.5}$ core (Figure 1B). These interactions are interligand and, thus, further link the $[H_5\mathbf{1}]^-$ ligands to create an H-bond macrocycle. The H-bonds occur between the αNH and α′NH groups from the urea on one $[H_5\mathbf{1}]^-$ ligand and the urea carbonyl moiety of the other tripodal ligand. The NH···O=C bonds are asymmetric: an

(14) Kryativ, S. V.; Nazarenko, A. Y.; Robinson, P. D.; Rybak-Akimova, E. V. *Chem. Commun.* **2000**, 921−222.
(15) Meyer, F.; Pritzkow, H. *Chem. Commun.* **1998**, 1555−1556.
(16) Cotton, F. A.; Ilsley, W. H.; Kaim, W. *J. Am. Chem. Soc.* **1980**, *102*, 3464−3474.
(17) For other examples of bridging cyclic ureate: (a) Doyle, M. P.; Zhou, Q.-L.; Raab, C. E.; Roos, G. H. P.; Simonsen, S. H.; Lynch, V. *Inorg. Chem.* **1996**, *35*, 6064−6073. (b) Raptopoulou, C. P.; Tangoulis, V.; Psycharis, V. *Inorg. Chem.* **2000**, *39*, 4452−4459.

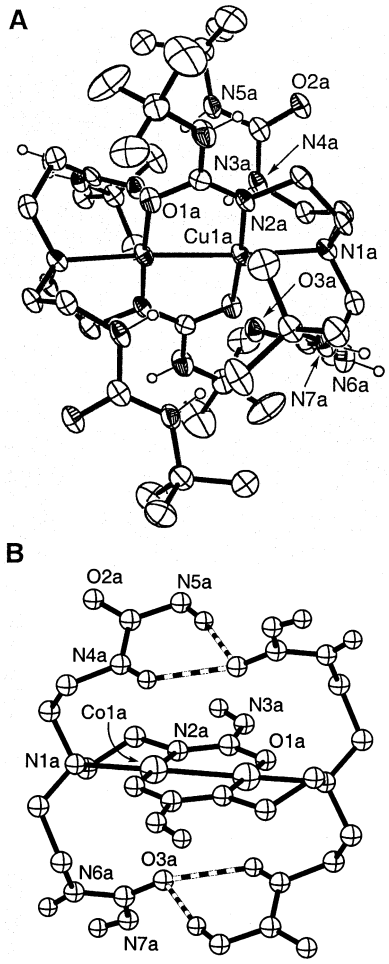

Figure 1. Thermal ellipsoid diagram of $[Cu(H_5\mathbf{1a})]_2^+$ (A) with the ellipsoids drawn at the 50% probability level and all non-urea hydrogens removed for clarity. Ball and stick diagram of $[Cu(H_5\mathbf{1a})]_2^+$ (B) showing the intramolecular H-bonds surrounding the $Cu^{1.5}Cu^{1.5}$ core. Only the urea hydrogens are shown, and the urea *tert*-butyl groups have been removed for clarity.

average N···O distance of 2.852(5) Å is observed for one H-bond, while the second interaction is at a distance of 3.131(5) Å. The resulting macrocycle places additional donor groups proximal to the axial coordination sites of copper center. For instance, a Cu1a···O3a distance of 3.049(4) Å is observed in $[Cu(H_5\mathbf{1a})]_2^+$ (Figure 1B). In addition, one urea N−H group is positioned near each copper ion. In $[Cu(H_5\mathbf{1a})]_2^+$ the Cu1a···N4a and Cu1a···H4a−N4a distances are 2.815(5) and 2.459(5) Å, respectively, and the Cu1a−H4a−N4a angle is 106°.[18] These metrical parameters are consistent with M···H hydrogen bonds, which are favored when the M···H bond lengths are shorter than the M···NH bond length and the M−H−N angle is greater than 100°.[19]

Probing $Cu^{1.5}Cu^{1.5}$ Core Formation: Preparation and Structure of $[CuH2]_2^+$. The structural properties of $[Cu(H_5\mathbf{1})]_2^+$ prompted us to consider the assembly of the mixed-valent dicopper core. In particular, we were interested in assessing whether the H-bonded macrocycle found in the solid state structure of $[Cu(H_5\mathbf{1})]_2^+$ was necessary to stabilize a $Cu^{1.5}Cu^{1.5}$ unit. This led us to investigate the formation of a mixed-valent dicopper complex with $H_2\mathbf{2}$, which has only one urea arm extending from the amine nitrogen. $[H\mathbf{2}]^-$ is similar to $[H_5\mathbf{1}]^-$ in that it has an ethylene spacer between the nitrogen atom of the amine and the αNH group of the urea, yet the opportunity for it to form a complex with intramolecular H-bonds, as in $[Cu(H_5\mathbf{1})]_2^+$, has been removed by permethylating the nitrogen atom of the amine.

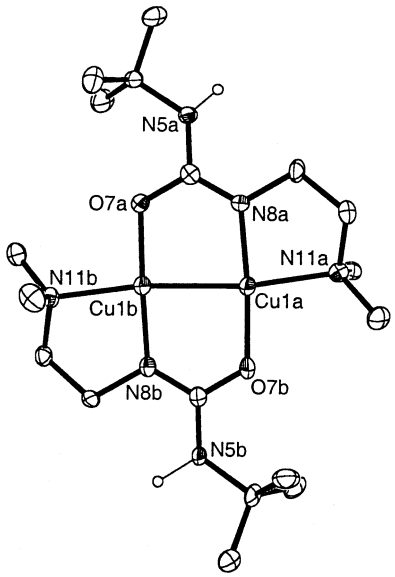

Figure 2. Thermal ellipsoid diagram of $[Cu(H\mathbf{2a})]_2^+$ with the ellipsoids drawn at the 50% probability level and all non-urea hydrogens removed for clarity.

$H_2\mathbf{2}$ readily forms a $Cu^{1.5}Cu^{1.5}$ complex. When the same synthetic protocols as used for $[Cu(H_5\mathbf{1})]_2^+$ were followed, a deep blue dicopper salt, formulated as $[Cu(H\mathbf{2})]_2BF_4$, was isolated in yields of greater than 70% (Scheme 1). $[Cu(H\mathbf{2})]_2BF_4$ crystallized in the $P\bar{1}$ space group, with three independent, but nearly identical, cations per asymmetric unit (denoted "a", "c", and "d"). Cations $[Cu(H\mathbf{2c})]_2^+$ and $[Cu(H\mathbf{2d})]_2^+$ sit on crystallographic centers of symmetry. The molecular structure of $[Cu(H\mathbf{2a})]_2^+$ is shown in Figure 2, and selected metrical parameters for all the cations are listed in Table 2. The dicopper core structures of the $[Cu(H\mathbf{2})]_2^+$ cations are the same as in $[Cu(H_5\mathbf{1})]_2^+$. Each copper ion in $[Cu(H\mathbf{2})]_2^+$ has a square planar coordination geometry, with two μ-1,3-(κN:κO)-ureate bridges. The Cu−N(O) bond lengths and angles in $[Cu(H\mathbf{2})]_2^+$ are comparable to those in $[Cu(H_5\mathbf{1})]_2^+$. For instance, $[Cu(H\mathbf{2a})]_2^+$ has an average Cu−Cu bond length of 2.3876(12) Å, which is only 0.0062 Å shorter than that found in $[Cu(H_5\mathbf{1})]_2^+$.

One noteworthy difference between the structures of the two dicopper complexes is the lack of intramolecular H-bonds in $[Cu(H\mathbf{2})]_2^+$. As expected, the removal of two urea arms in $[H\mathbf{2}]^-$ eliminates intramolecular H-bonds. However, it is clear that the assembly of the $Cu^{1.5}Cu^{1.5}$ core still occurs in $[Cu(H\mathbf{2})]_2^+$, suggesting that the H-bonds are not needed to stabilize this type of structural motif. The two μ-1,3-(κN:κO)-ureate bridges and five-membered chelate rings (those including the amine nitrogen atom and αN$^-$)

(18) Similar structural results are found for $[Cu(H_5\mathbf{1b})]_2^+$: Cu1b···O3b, 3.010(4) Å; Cu1b···N4b, 2.843(5) Å; Cu1b···H4b−N4b, 2.503(5) Å; Cu1b−H4b−N4b, 104°.

(19) Braga, D.; Grepioni, F.; Tedesco, E.; Biradha, K.; Desiraju, G. R. *Organometallics* **1997**, *16*, 1846−1852 and references therein.

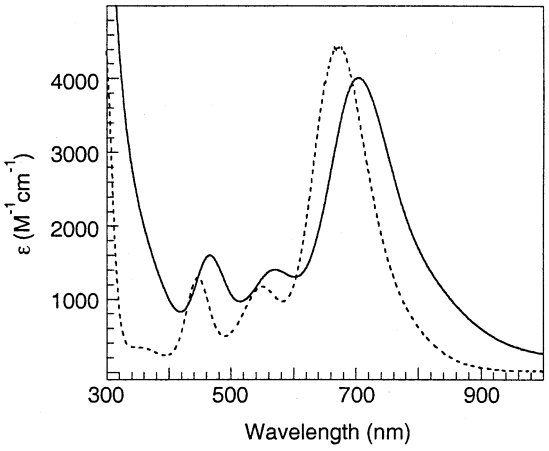

Figure 3. Electronic absorbance spectra of $[Cu(H_5\mathbf{1})]_2^+$ (—) and $[Cu(H\mathbf{2})]_2^+$ (- - -) recorded in CH_2Cl_2 at room temperature.

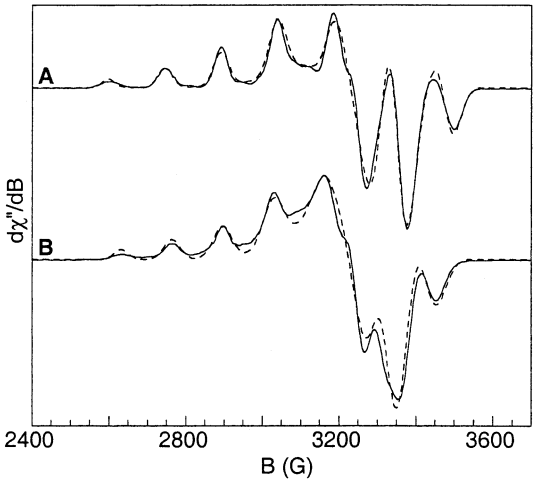

Figure 4. X-band (9.3 GHz) EPR spectra of $[Cu(H\mathbf{2})]_2^+$ (A) and $[Cu(H_5\mathbf{1})]_2^+$ (B) in frozen solutions (1 mM, THF) at 77 K. Solid line spectra are experimental data, and dash line spectra are simulations with parameters given in text.

appear to be the main contributors in the assembly of these mixed-valent dicopper complexes.

Spectroscopic Properties of $[Cu(H_5\mathbf{1})]_2^+$ and $[Cu(H\mathbf{2})]_2^+$. The two mixed-valent dicopper complexes have nearly identical spectroscopic properties. The electronic absorbance spectra for $[Cu(H_5\mathbf{1})]_2^+$ and $[Cu(H\mathbf{2})]_2^+$ are presented in Figure 3. For $[Cu(H_5\mathbf{1})]_2^+$, the visible spectrum contains an intense band at 705 nm ($\epsilon_M = 4000$) and two weaker, lower energy signals at 568 ($\epsilon_M = 1400$) and 466 nm ($\epsilon_M = 1600$). These bands are slightly blue shifted in the spectrum of $[Cu(H\mathbf{2})]_2^+$ to 672 ($\epsilon_M = 4420$), 549 ($\epsilon_M = 1170$), and 446 nm ($\epsilon_M = 1300$). $[Cu(H\mathbf{2})]_2^+$ has an additional transition at 360 nm ($\epsilon_M = 320$). The electronic absorbance spectra for $[Cu(H_5\mathbf{1})]_2^+$ and $[Cu(H\mathbf{2})]_2^+$ resemble those found in other type III mixed-valent copper dimers; in particular, the complexes with octaazacryptate ligands. These complexes, which contain all nitrogen donors and five-coordinate copper centers, have two absorbance features that range from 600 to 650 nm ($\epsilon_M = 1500-3500$) and 720−850 nm ($\epsilon_M = 5000$). The lower energy bands in these complexes have been assigned as a $\psi \rightarrow \psi^*$ transition from the $Cu^{1.5}Cu^{1.5}$ manifold.[20] A similar transition could give rise to the absorbance bands at ∼700 nm in $[Cu(H_5\mathbf{1})]_2^+$ and $[Cu(H\mathbf{2})]_2^+$, because of the similar spectral properties between these urea bridge dimers and those made with octaazacryptates.[4]

The X-band EPR spectra for $[Cu(H_5\mathbf{1})]_2^+$ and $[Cu(H\mathbf{2})]_2^+$ measured at 77 K and their corresponding simulated spectra are presented in Figure 4. Type III mixed-valent copper complexes have distinctive EPR properties, which include seven-line hyperfine coupling from the unpaired electron interacting with two $I = {}^3/_2$ copper centers and temperature-independent delocalization.[4−6,20,21] These EPR features are found for $[Cu(H_5\mathbf{1})]_2^+$ and $[Cu(H\mathbf{2})]_2^+$, supporting their assignments as fully delocalized mixed-valent species. Both complexes show a 7-line EPR signal at 77 K (Figure 4), and the same at 4 K (Figure S4, Supporting Information). There are additional lines with significantly weaker intensity from the same spin system that are not well resolved in these complexes, but are better resolved in other complexes.[6a−c,21] Simulations of the 77 K spectrum for $[Cu(H_5\mathbf{1})]_2^+$ determined a **g**-tensor of $g = 2.023, 2.070, 2.197$ with corresponding hyperfine coupling constants of $A = 14, 38, 132$ G. Similar values were found for $[Cu(H\mathbf{2})]_2^+$: $g = 2.018, 2.077, 2.188$, and $A = 15, 53, 147$ G. The g and A values obtained for $[Cu(H_5\mathbf{1})]_2^+$ and $[Cu(H\mathbf{2})]_2^+$ are typical of those reported for other fully delocalized mixed-valent copper complexes.[6]

Electrochemical Properties. The redox properties of $[Cu(H_5\mathbf{1})]_2^+$ and $[Cu(H\mathbf{2})]_2^+$ were examined by cyclic voltammetry. Both complexes show irreversible reductive processes near −1.0 V vs SCE when recorded at scan rates between 0.100 and 1.00 V s^{-1}. Additional irreversible oxidative peaks were found at 0.33 V vs SCE for $[Cu(H_5\mathbf{1})]_2^+$ and 0.71 V vs SCE for $[Cu(H\mathbf{2})]_2^+$. The difference of nearly 0.4 V between these two E_{pa} values could reflect the distinct microenvironment that surrounds the dicopper cores in each complex. In $[Cu(H\mathbf{2})]_2^+$, the $Cu^{1.5}Cu^{1.5}$ unit is exposed because the $[H\mathbf{2}]^-$ ligands do not have extra urea arms to confine the copper centers. In addition, $[H\mathbf{2}]^-$ does not have additional functional groups that can interact with the metal centers. By contrast, the $Cu^{1.5}Cu^{1.5}$ unit in $[Cu(H_5\mathbf{1})]_2^+$ is confined within the H-bonded macrocycle (vide supra), which controls the space around the vacant axial sites on the copper centers. The lower oxidation potential in $[Cu(H_5\mathbf{1})]_2^+$ results, in part, from placing additional donors (e.g., oxygen atoms of urea carbonyl groups) within ∼3.0 Å from the dinuclear copper core.

Summary

This work describes the synthesis of new mixed-valent copper complexes, $[Cu(H_5\mathbf{1})]_2^+$ and $[Cu(H\mathbf{2})]_2^+$. These complexes have fully delocalized dicopper cores, which are supported by structural and spectroscopic results. Both

(20) (a) Farrar, J. A.; Grinter, R.; Neese, F.; Nelson, J.; Thomson, A. J. *J. Chem. Soc., Dalton Trans.* **1997**, 4083−4087. (b) Gamelin, D. R.; Randall, D. W.; Hay, M. T.; Houser, R. P.; Mulder, T. C.; Canters, G. W.; de Vries, S.; Tolman, W. B.; Lu, Y.; Solomon, E. I. *J. Am. Chem. Soc.* **1998**, *120*, 5246−5263.

(21) Antholine, W. E.; Kastrau, D. H. W.; Steffens, G. C. M.; Buse, G.; Zumft, W. G.; Kroneck, P. M. H. *Eur. J. Biochem.* **1992**, *209*, 875−881.

complexes have Cu−Cu distances of ∼2.39 Å; these distances are shorter that those found in most other dinuclear copper complexes. The short Cu−Cu distances in $[Cu(H_5\mathbf{1})]_2^+$ and $[Cu(H\mathbf{2})]_2^+$ result from two μ-1,3-(κN:κO)-ureate bridges between the copper centers. In $[Cu(H_5\mathbf{1})]_2^+$, the $Cu^{1.5}Cu^{1.5}$ core is enclosed within a pseudomacrocycle that is formed via intramolecular H-bonds between adjacent urea groups. However, this macrocycle is not required to isolate the $Cu^{1.5}Cu^{1.5}$ core. $[Cu(H\mathbf{2})]_2^+$, which is unable to form a macrocycle, was readily prepared and has a copper core structure indistinguishable from that of $[Cu(H_5\mathbf{1})]_2^+$. These results demonstrate the utility of μ-1,3-(κN:κO)-ureate bridges in assembling polynuclear metal complexes.

Acknowledgment is made to the NIH (GM50781 to A.S.B.; GM49970 to M.P.H) for financial support of this research. The X-ray diffraction instrumentation was purchased with funds from the National Science Foundation (CHE-0079282) and the University of Kansas.

Supporting Information Available: CIF files of X-ray structural data, thermal ellipsoid plots of $[H_3\mathbf{2}]BF_4$ (Figure S1), $[Cu(H_5\mathbf{1b})]_2^+$ (Figure S2), and $[Cu(H\mathbf{2c})]_2^+$ and $[Cu(H\mathbf{2d})]_2^+$ (Figure S3), and EPR spectra of $[Cu(H_5\mathbf{1})]_2^+$ and $[Cu(H\mathbf{2})]_2^+$ recorded at 4 K (Figure S4). This material is available free of charge via the Internet at http://pubs.acs.org.

IC0202918